The integrals in Eq. (3) can be discretized using the trapezoidal rule to give

$$\phi_{J,k}(n\Delta t) = \frac{\lambda}{2}\,[U_{kk}^{(1)}(\Delta t) + U_{kk}^{(1)}(0)]\phi_{J-1,k}(n\Delta t) + G \qquad (6)$$

where G is a term that is composed of values of $\phi_{J-1,j}$ at previous time steps. There are n time steps of Δt. The factor λ is introduced to allow for different kinds of boundary conditions. If $\lambda = 0$, then Eq. (6) represents an explicit boundary condition, because it is composed only of values at previous time steps. If $\lambda = 1$, then the boundary condition includes terms at the current time step. A fractional value of λ represents an intermediate situation, for example, if the boundary condition is applied after the first sweep of an alternating-direction implicit algorithm.

Results

The example chosen is a NACA 64A010 airfoil, oscillating in pitch about zero angle of attack, at a reduced frequency ν of 0.1, an amplitude of 1 deg, and at a freestream Mach number of 0.8.

In Fig. 2, results of the present method applied at $x = 1.12$, 1.35, and 1.75 are shown with the expected result that the larger the computation domain the more accurate the result. These results are compared with the standard result, that is, the result computed using XTRAN2L[5] in its standard mode. Also shown is the result using the standard method on the truncated grid; in this case and the present method, the grid is truncated at $x = 1.35$ compared with the standard grid boundary at $x = 21$. The airfoil trailing edge is at $x = 1$. The standard method for the truncated grid diverges at 150 time steps; in this case the shock wave is located at the trailing edge compared with the correct location at about 50% chord. It is important to note that even the largest domain shown here extends behind the airfoil only approximately 4% of the extent of the standard grid.

Concluding Remarks

A novel method of computing boundary conditions for unsteady flow computations has been derived and tested for the unsteady transonic small disturbance equations. The results indicate that computational domains could be reduced considerably if this technique were used. There is no difficulty in principle in applying the present ideas to more complex equations, such as the Euler or Navier-Stokes equations.

Acknowledgment

This work was supported by the Air Force Office of Scientific Research under Contract F49620-88-C-0006.

References

[1]Hedstrom, G. W., "Nonreflecting Boundary Conditions for Nonlinear Hyperbolic Systems," *Journal of Computational Physics,* Vol. 30, No. 2, 1979, pp. 222–237.

[2]Thompson, K. W., "Time Dependent Boundary Conditions for Hyperbolic Systems," *Journal of Computational Physics,* Vol. 68, No. 1, 1987, pp. 1–24.

[3]Rodman, L. C., "The Application of Non-Reflecting Boundary Conditions to 2-D Unsteady Computations on Curvilinear Grids," AIAA Paper 90-1587, June 1990.

[4]Nixon, D., and Tzuoo, K.-L., "Prediction of Gust Loading and Alleviation at Transonic Speeds," *Journal of Aircraft,* Vol. 24, No. 10, 1987, pp. 703–709.

[5]Whitlow, W., "XTRAN2L—A Program for Solving the General Frequency Unsteady Transonic Small Disturbance Equation," NASA TM 85223, 1983.

Alternating Direction Implicit Methods for the Navier-Stokes Equations

T. L. Tysinger* and D. A. Caughey†
Cornell University, Ithaca, New York 14853

I. Introduction

In the numerical simulation of viscous flows at high Reynolds numbers, it is necessary to resolve the thin shear layers that develop near solid boundaries. Such thin shear regions require the use of grids with cells of very high aspect ratio, which are known to hinder convergence for steady problems when using explicit schemes. To overcome these difficulties, Caughey has developed a diagonal alternating direction implicit (ADI) algorithm for the solution of the Euler equations of inviscid, compressible flow.[1] Rapid convergence is achieved with the use of the implicit scheme within a multigrid framework.

Here, the method is extended to solve the Navier-Stokes equations. Attention is focused on methods of adding the viscous contributions in a way that does not disturb the overall stability and efficiency of the implicit scheme. No attempt is made here to incorporate a turbulence model, so the discussion will be limited to laminar flows.

II. Governing Equations

Compressible viscous flows are governed by the Navier-Stokes equations. These equations require that both streamwise and normal viscous diffusion be computed. The nondimensionalized form of the full Navier-Stokes (FNS) equations is written in curvilinear coordinates as

$$\frac{\partial \underline{W}}{\partial t} + \frac{\partial \underline{F}_C}{\partial \xi} + \frac{\partial \underline{G}_C}{\partial \eta} = \frac{\partial \underline{F}_V}{\partial \xi} + \frac{\partial \underline{G}_V}{\partial \eta} \qquad (1)$$

where $\underline{W}$ is the transformed dependent variable, $\underline{F}_C(\underline{W})$ and $\underline{G}_C(\underline{W})$ are the convective flux vectors, and $\underline{F}_V(\underline{W}, \underline{W}_\xi, \underline{W}_\eta)$ and $\underline{G}_V(\underline{W}, \underline{W}_\xi, \underline{W}_\eta)$ are the viscous flux vectors. An equation of state is used to relate the pressure to the total energy.

Under conditions in which the flow has a predominant direction and is without massive separation, it is possible to neglect viscous diffusion in the streamwise direction without adversely affecting the quality of the solution. This results in the so-called thin layer approximation (TLA).

The viscous flux vectors can be decoupled into components that depend only on the vector of dependent variables and its derivative in either the ξ or η direction:

$$\underline{F}_V = \underline{F}_V(\underline{W}, \underline{W}_\xi, \underline{W}_\eta) = \underline{\tilde{F}}_V(\underline{W}, \underline{W}_\xi) + \underline{\hat{F}}_V(\underline{W}, \underline{W}_\eta) \qquad (2)$$

$$\underline{G}_V = \underline{G}_V(\underline{W}, \underline{W}_\xi, \underline{W}_\eta) = \underline{\tilde{G}}_V(\underline{W}, \underline{W}_\xi) + \underline{\hat{G}}_V(\underline{W}, \underline{W}_\eta) \qquad (3)$$

The TLA entails retaining only the surface normal or η derivatives in the viscous terms of the Navier-Stokes equations [Eq.

Presented as Paper 91-0242 at the AIAA 29th Aerospace Sciences Meeting, Reno, NV, Jan. 7–10, 1991; received March 11, 1991; revision received Dec. 12, 1991; accepted for publication Dec. 13, 1991. Copyright © 1990 by the American Institute of Aeronautics and Astronautics, Inc. All rights reserved.

*Graduate Research Assistant; currently, Research Scientist, Fluent, Inc., Lebanon, NH. Member AIAA.

†Professor, Sibley School of Mechanical and Aerospace Engineering. Associate Fellow AIAA.

(1)]; that is, only the term $\hat{G}_V(\underline{W}, \underline{W}_\eta)$ is kept when the body surface is a line of constant η. The TLA equations are then written

$$\frac{\partial \underline{W}}{\partial t} + \frac{\partial \underline{F}_C}{\partial \xi} + \frac{\partial \underline{G}_C}{\partial \eta} = \frac{\partial \hat{\underline{G}}_V}{\partial \eta} \tag{4}$$

III. Numerical Method

Spatial discretization of the governing equations is accomplished with a finite volume scheme similar to that of Jameson et al.[2] To prevent oscillations in regions where the grid is incapable of resolving the gradients, such as near shocks, adaptive dissipation similar to that described by Jameson et al.[2] and modified by Caughey[1] is added to the scheme.

For problems in which only the steady-state solution is of interest, local time stepping is applied. A full multigrid algorithm based on that originally developed by Jameson[3] and described by Caughey[1] and Smith and Caughey[4] is implemented to further accelerate convergence.

To advance the solution in time, an ADI procedure suitable for the Navier-Stokes equations has been developed. Attention here is directed at methods to include viscous contributions in the implicit operators. Only the TLA equations are considered in this analysis. Further details, including a derivation appropriate for the full Navier-Stokes equations, can be found in Ref. 5.

The scheme begins by approximating spatial derivatives at new and old time levels, linearizing the changes in the flux vectors, and approximating the implicit operator as a product of one-dimensional factors. Linearization of the convective flux vectors introduces the Jacobians, $A = (\partial \underline{F}_C / \partial \underline{W})$ and $B = (\partial \underline{G}_C / \partial \underline{W})$.[6-8] Since the transformed viscous flux $\hat{\underline{G}}_V$ is a function of $\underline{W}$ and $\underline{W}_\eta$, the appropriate linearization introduces two additional Jacobians, $\hat{M} = (\partial \hat{\underline{G}}_V / \partial \underline{W})$ and $\hat{N} = (\partial \hat{\underline{G}}_V / \partial \underline{W}_\eta)$. If the transport coefficients and metrics are approximated to be locally constant, $\hat{M} - \hat{N}_\eta \equiv O$ (Refs. 9 and 10), and only the Jacobian with respect to the derivatives of the solution, $\hat{N}$, is needed. This matrix contains no derivatives of the solution variables, unlike the coefficient matrix in Ref. 11 in which the metrics are not approximated as locally constant. Such linearization in the implicit operators results in a block pentadiagonal system of equations when the fourth differences due to the numerical dissipation are included.

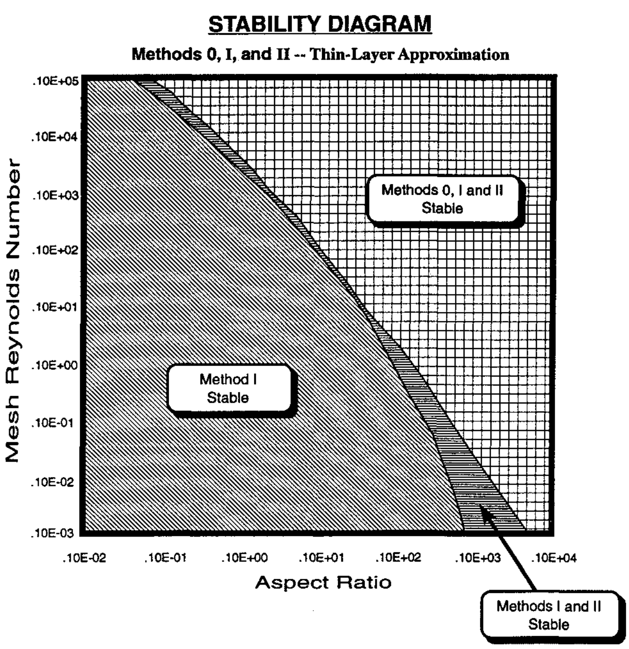

Fig. 1 Regions of linear stability for methods 0, I, and II; shaded areas represent regions of stability where the magnitude of the growth factor is less than unity.

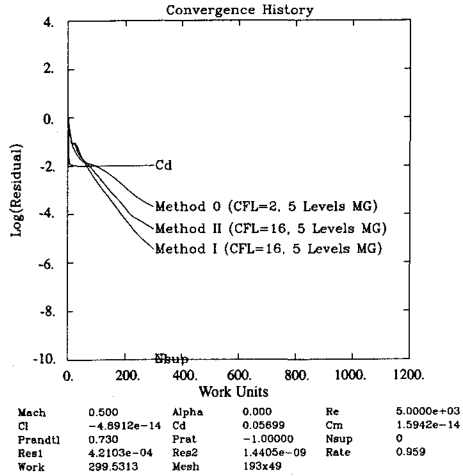

Fig. 2 Convergence histories using multigrid; $Re = 5 \times 10^3$, $M_\infty = 0.50$, $\alpha = 0.0$, methods I and II at Courant number 16, method 0 at Courant number 2.

For the Euler equations, the convective flux Jacobians can be diagonalized with local similarity transformations as $A = Q_A \Lambda_A Q_A^{-1}$ and $B = Q_B \Lambda_B Q_B^{-1}$, where Λ_A and Λ_B are diagonal matrices whose diagonal elements are the eigenvalues of their respective Jacobians, and Q_A and Q_B are the modal matrices whose elements can be found in Ref. 8. This allows the block system to be decoupled into equations that can be solved as scalar pentadiagonal systems, greatly reducing the amount of computational labor needed for a solution.

For the Navier-Stokes equations, it is not possible both to include the viscous terms in the implicit factor and to diagonalize the system, since the convective and viscous Jacobians are not simultaneously diagonalizable. Several alternatives exist to circumvent this problem.

One alternative is to neglect the viscous contributions completely from implicit consideration but maintain their contribution to the explicit residual. For bookkeeping, this explicit treatment will be called method 0. Neglecting the viscous terms from the implicit factors may jeopardize the stability of the scheme. It is desirable to maintain the efficiency of the diagonalized scheme without degrading its stability properties, so two alternate implicit methods are explored.

Method I: Implicit Approximation

The first implicit method uses the largest eigenvalue of the viscous Jacobian to add contributions to the inviscid implicit factors. This is similar to what was suggested by Pulliam.[12] The eigenvalues of $\hat{N}$ are

$$\begin{aligned}
\lambda_1 &= \left(\frac{2\mu + \lambda}{\rho}\right)(\eta_x^2 + \eta_y^2) \\
\lambda_2 &= \left(\frac{\gamma\mu}{\rho Pr}\right)(\eta_x^2 + \eta_y^2) \\
\lambda_3 &= \left(\frac{\mu}{\rho}\right)(\eta_x^2 + \eta_x^2) \\
\lambda_4 &= 0
\end{aligned} \tag{5}$$

where Pr is the Prandtl number, μ and λ are the viscosity coefficients, and γ is the ratio of specific heats.

The scheme is constructed by adding the diagonal approximations $\hat{\Lambda}_{\hat{N}} \approx Q_B^{-1} \hat{N} Q_B$ to the appropriate implicit factor:

$$\begin{aligned}
&(I + \theta \Delta t \Lambda_{Aij} \delta_\xi) Q_{Aij}^{-1} \\
&\times Q_{Bij} [I + \theta \Delta t (\Lambda_{Bij} \delta_\eta - \delta_\eta^2 \hat{\Lambda}_{\hat{N}ij})] Q_{Bij}^{-1} \Delta \underline{W}_{ij}^n \\
&= -\Delta t Q_{Aij}^{-1} (\delta_\xi \underline{F}_{Cij}^n + \delta_\eta \underline{G}_{Cij}^n - \delta_\eta \hat{\underline{G}}_{Vij}^n)
\end{aligned} \tag{6}$$

The diagonal approximation $\hat{\Lambda}_{\hat{N}}$ is, for example,

$$\hat{\Lambda}_{\hat{N}} = \lambda_2 I = \left(\frac{\gamma\mu}{\rho Pr}\right)(\eta_x^2 + \eta_y^2)I \qquad (7)$$

where I is the identity matrix. For simplicity, the terms arising from the artificial dissipation are not shown in the equations. The number of additional operations needed to implement this scheme is negligible since it involves only the calculation of an eigenvalue whose analytical form is known.

Method II: Additional Operator

A second option is to use additional implicit operators that contain the exclusive contributions from the viscous terms. The addition of the viscous Jacobians directly to the operators would require the solution of block tridiagonal systems. However, since the eigenvalues of the viscous Jacobians are distinct [Eqs. (5)], a modal matrix $Q_{\hat{N}}$ exists that diagonalizes $\hat{N}$ through a similarity transformation. This results in the diagonal scheme

$$\begin{aligned} &(I + \theta\Delta t \Lambda_{Aij}\delta_\xi)Q_{Aij}^{-1} \times Q_{Bij}(I + \theta\Delta t\Lambda_{Bij}\delta_\eta)Q_{Bij}^{-1} \\ &\times Q_{\hat{N}ij}(I - \theta\Delta t\delta_\eta^2\Lambda_{\hat{N}ij})Q_{\hat{N}ij}^{-1}\Delta \underline{W}_{ij}^n \\ &= -\Delta t Q_{Aij}^{-1}(\delta_\xi \underline{F}_{Cij}^n + \delta_\eta \underline{G}_{Cij}^n - \delta_\eta \hat{\underline{G}}_{Vij}^n) \end{aligned} \qquad (8)$$

where $\Lambda_{\hat{N}ij} = Q_{\hat{N}ij}^{-1}\hat{N}Q_{\hat{N}ij}$ is the diagonal matrix whose nonzero elements are the eigenvalues of $\hat{N}$. In this scheme, an additional scalar tridiagonal system must be solved; for the full Navier-Stokes approximation, two additional factors appear in the equation. The viscous modal matrices are written

$$Q_{\hat{N}} = \begin{bmatrix} 0 & 0 & 0 & 1 \\ \tilde{\eta}_x & 0 & \tilde{\eta}_y & u \\ \tilde{\eta}_y & 0 & -\tilde{\eta}_x & v \\ \tilde{\theta} & 1 & -\tilde{\mu} & e/\rho \end{bmatrix} \qquad (9)$$

$$Q_{\hat{N}}^{-1} = \begin{bmatrix} -\dfrac{\tilde{\theta}}{\tilde{\eta}_x^2 + \tilde{\eta}_y^2} & \dfrac{\tilde{\eta}_x}{\tilde{\eta}_x^2 + \tilde{\eta}_y^2} & \dfrac{\tilde{\eta}_y}{\tilde{\eta}_x^2 + \tilde{\eta}_y^2} & 0 \\ -\dfrac{e}{\rho} + u^2 + v^2 & -u & -v & 1 \\ \dfrac{\tilde{\mu}}{\tilde{\eta}_x^2 + \tilde{\eta}_y^2} & \dfrac{\tilde{\eta}_y}{\tilde{\eta}_x^2 + \tilde{\eta}_y^2} & -\dfrac{\tilde{\eta}_x}{\tilde{\eta}_x^2 + \tilde{\eta}_y^2} & 0 \\ 1 & 0 & 0 & 0 \end{bmatrix} \qquad (10)$$

where

$$\tilde{\eta}_x = \frac{\eta_x}{\sqrt{\eta_x^2 + \eta_y^2}}, \qquad \tilde{\eta}_y = \frac{\eta_y}{\sqrt{\eta_x^2 + \eta_y^2}}$$

$$\tilde{\theta} = \tilde{\eta}_x u + \tilde{\eta}_y v, \qquad \tilde{\mu} = \tilde{\eta}_x v - \tilde{\eta}_y u$$

Stability Analysis

Some insight into the stability properties of these schemes is obtained from a von Neumann (Fourier) analysis of an advection-diffusion equation. This equation with fourth-order numerical dissipation is written

$$\frac{\partial u}{\partial t} + c\frac{\partial u}{\partial x} + c\frac{\partial u}{\partial y} + c\epsilon\Delta x^3\frac{\partial^4 u}{\partial x^4} + c\epsilon\Delta y^3\frac{\partial^4 u}{\partial y^4} = \nu\frac{\partial^2 u}{\partial y^2} \qquad (11)$$

This equation serves as a model for the TLA of the Navier-Stokes equations. Substituting the Fourier term $u_{ij}^n = G^n e^{i\beta_x x}e^{i\beta_y y}$ and constructing an ADI scheme analogous to that described earlier leads to an equation for the growth factor G. In addition to the Courant number and artificial dissipation ϵ, the numerical stability of the implicit viscous equations is governed primarily by the aspect ratios of the mesh cells and the mesh Reynolds numbers.

Using such a model, it is found that, when viscous terms are added directly to the convective operators, analogous to what is done with method I, unconditional stability is achieved. If the viscous terms are evaluated explicitly without implicit contributions (analogous to method 0), a conditionally stable scheme results. This can be seen in Fig. 1 in which the shaded areas represent regions in parameter space where von Neumann analysis predicts an amplification factor less than unity. This figure represents the properties of the scheme applied to a model problem using values of the dissipation parameters representative of those used in the computations and a Courant number of 16. These results do not rule out the possibility of obtaining a converged solution without including viscous contributions in the implicit factors. If additional viscous operators are added to the scheme (as is done in method II), the solution will only remain conditionally stable, although the region of stability is increased slightly, relative to method 0, as shown in Fig. 1. The stability analysis indicates that the most promising algorithm would be one similar to method I. Method II should also be considered, however, insofar as it represents less of an ad hoc approximation than method I.

IV. Results and Conclusions

To illustrate the effect of the implicit methods, a subcritical laminar flow ($Re = 5 \times 10^3$, $M_\infty = 0.5$) past a two-dimensional NACA 0012 symmetric airfoil at zero degrees incidence is calculated. A 192×48 cell "C" grid is used. A full multigrid scheme is used with the solution on the coarsest grid initialized to freestream values. Plots of the convergence histories for the different methods on the finest grid are shown in Fig. 2. Five levels of multigrid and local time stepping are used for the results. The error curves plotted are the normalized root mean square of the density residual. Using method I with multigrid, the solution converged to a steady state in approximately 35 work units, which is 20 multigrid cycles. One work unit is defined as the amount of work required to advance the solution one timestep on the finest grid level; for a simple V cycle, the strategy used here, each multigrid cycles requires approximately 1-2/3 work units.

At a Courant number of 16, both methods I and II produce converged solutions as illustrated in Fig. 2. The asymptotic convergence of method I is somewhat better than that of method II. A converged solution is not attainable if viscous terms are neglected from the implicit factors (method 0) at Courant number of 16. However, the scheme does converge at the expense of a lower Courant number, hence, a slower convergence rate, as shown in Fig. 2. This demonstrates the importance of maintaining an implicit viscous contribution in the numerical scheme.

The importance of including viscous contributions in the implicit operator has been demonstrated. Although several options are available for implicit inclusion, the addition of approximate terms to the existing operators (method I) seems the most effective.

Acknowledgments

This research has been supported in part by the Independent Research and Development Program of the McDonnell Douglas Corporation and by the NASA Ames Research Center under Grant NAG 2-665. The calculations reported here were performed at the Cornell National Supercomputer Facility, a resource of the Cornell Theory Center, which receives major funding from the National Science Foundation and the IBM Corporation, with additional support from New York State and the Corporate Research Institute.

References

[1]Caughey, D. A., "Diagonal Implicit Multigrid Algorithm for the Euler Equations," *AIAA Journal*, Vol. 26, No. 7, 1988, pp. 841-851.

[2]Jameson, A., Schmidt, W., and Turkel, E., "Numerical Solutions

of the Euler Equations by Finite Volume Methods Using Runge-Kutta Time-Stepping Schemes," AIAA Paper 81-1259, Palo Alto, CA, June 23-25, 1981.

[3]Jameson, A., "Solution of the Euler Equations by a Multigrid Method," Dept. of Mechanical and Aerospace Engineering, Princeton, Univ., MAE Rept. 1613, Princeton, NJ, June 1983.

[4]Smith, W. A., and Caughey, D. A., "Multigrid Solution of Inviscid Transonic Flow Through Rotating Blade Passages," AIAA 25th Aerospace Sciences Meeting, AIAA Paper 87-0608, Reno, NV, Jan. 12-15, 1987.

[5]Tysinger, T. L., and Caughey, D. A., "Implicit Multigrid Algorithm for the Navier-Stokes Equations," AIAA 29th Aerospace Sciences Meeting, AIAA Paper 91-0242, Reno, NV, Jan. 7-10, 1991.

[6]Warming, R. F., Beam, R. M., and Hyett, B. J., "Diagonalization and Simultaneous Symmetrization of the Gas Dynamic Equations," *Mathematics of Computation*, Vol. 29, 1975, pp. 1037-1045.

[7]Beam, R. M., and Warming, R. F., "An Implicit Finite-Difference Algorithm for Hyperbolic Systems in Conservation Law Form," *Journal of Computational Physics*, Vol. 22, Sept. 1976, pp. 87-110.

[8]Chaussee, D. S., and Pulliam, T. H., "Two-Dimensional Inlet Simulation Using a Diagonal Implicit Algorithm," *AIAA Journal*, Vol. 19, No. 2, 1981, pp. 153-159.

[9]Beam, R. M., and Warming, R. F., "An Implicit Factored Scheme for the Compressible Navier-Stokes Equations," *AIAA Journal*, Vol. 16, No. 4, 1978, pp. 393-402.

[10]Peyret, R., "Finite-Difference and Finite-Volume Methods for the Computation of Compressible Viscous Flows," *Computational Fluid Dynamics*, Lecture Notes, Von Kármán Inst. for Fluid Dynamics Lecture Series, Brussels, Belgium, March 3-7, 1986.

[11]Steger, J. L., "Implicit Finite-Difference Simulation of Flow About Arbitrary Two-Dimensional Geometries," *AIAA Journal*, Vol. 16, No. 7, 1978, pp. 679-686.

[12]Pulliam, T. H., "Efficient Solution Methods for the Navier-Stokes Equations," *Numerical Techniques for Viscous Flow Computation in Turbomachinery Bladings*, Lecture Notes for Viscous Flow Computation in Turbomachinery Bladings, Brussels, Belgium, Jan. 20-24, 1986.

Modified k-ϵ Model for Compressible Free Shear Flows

C. P. Brescianini*

University of Queensland,

Brisbane, Queensland 4072, Australia

Introduction

IN the landmark conference on turbulent free shear flows, held at the NASA Langley Research Center in 1972,[1] the k-ϵ model emerged as one of the most capable of the turbulence models available at the time.[2] However, one deficiency of the k-ϵ model was also brought to light. Namely, the inability to predict the experimentally observed[3] decrease in the spreading rate of turbulent, supersonic, free shear layers as the Mach number was increased. A modification to the k-ϵ model is proposed here that helps remove this deficiency.

Theory

Modifications to the k-ϵ model to account for compressibility effects have been proposed in the past by Dash et al.[4] and Chuech et al.,[5] among others. Sarkar et al.[6] and Zeman[7] have recently proposed dissipation models that account for compressibility effects. The adaptation of these ideas to the k-ϵ model is also straightforward. An alternative approach is presented here, based on a recent suggestion by Kim.[8]

Received May 9, 1991; revision received Nov. 4, 1991; accepted for publication Nov. 5, 1991. Copyright © 1992 by the American Institute of Aeronautics and Astronautics, Inc. All rights reserved.

*Graduate Student, Department of Mechanical Engineering.

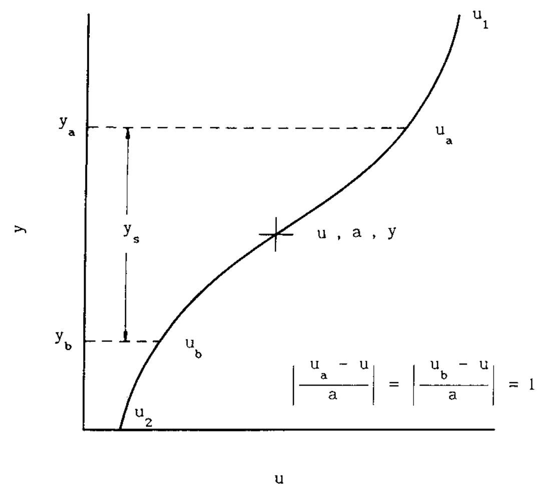

Fig. 1 Characteristic width for supersonic shear layers.[8]

Kim proposed a simple modification to another turbulence model, the Prandtl mixing length hypothesis (MLH). The MLH involves evaluating the turbulent viscosity by using a "mixing length" ℓ_m. This mixing length is usually computed by setting it equal to a constant fraction of some characteristic width y_G such that

$$\ell_m = \lambda y_G \tag{1}$$

where λ is a constant. For incompressible free shear layers, y_G is customarily taken as the width of the shear layer b, usually defined as

$$y_G = b + |y_{0.9} - y_{0.1}| \tag{2}$$

where at $y_{0.1}$, $u^* = 0.1$, and at $y_{0.9}$, $u^* = 0.9$, where $u^* = (u - u_2)/(u_1/ - u_2)$. Here u is the velocity, y is the transverse distance, and the subscripts 1 and 2 represent the high and low velocity sides of the shear layer, respectively.

Kim, however, proposed a modified formula and a different characteristic width y_s defined by

$$y_s = |y_a - y_b| \tag{3}$$

The locations of y_a and y_b were defined by points where sonic flow exists relative to the local point, as shown in Fig. 1. (In Fig. 1 a is the local speed of sound.) Limitations were placed on y_a and y_b in that these locations could not exceed the edges of the shear layer.

In the "standard" high Reynolds number k-ϵ model (designated the $k\epsilon 1$ model in Ref. 2), the turbulent viscosity is computed from

$$\mu_t = C_\mu \rho \left(\frac{k^2}{\epsilon}\right) \tag{4}$$

where C_μ is a constant, ρ is the density, k is the turbulent kinetic energy, and ϵ is the turbulent kinetic energy dissipation rate. The values for k and ϵ are determined by solving a pair of partial differential transport equations. Comparing Eq. (4) with the Prandtl-Kolmogorov formula

$$\mu_t = \rho\sqrt{k}\,\ell \tag{5}$$

where ℓ is the length scale, shows that the length scale used in the $k\epsilon 1$ model is determined from the relationship

$$\ell_\epsilon = C_\mu \frac{k^{1.5}}{\epsilon} \tag{6}$$